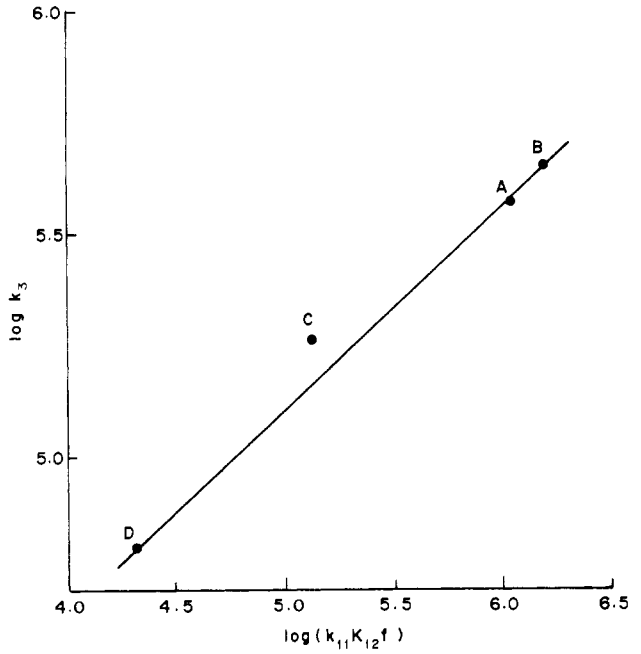

Figure 2. Plot of log k_3 vs log ($k_{11}K_{12}f$) for the oxidation of $[Ni^{II}(cyclam)]^{2+}$ by copper(III) imine–oxime complexes: (A) $[Cu^{III}L^1]^+$; (B) $[Cu^{III}L^2]^+$; (C) $[Cu^{III}L^3]^+$; (D) $[Cu^{III}L^4]^+$.

redox couples of each reagent, Z is the collision frequency in solution, usually taken as 10^{11} s^{-1}, and f is given by the expression in eq 15. This form of the Marcus relationship was found to be suitable for reactions between redox couples of the same charge type, as the reactions described here, because the work terms to a large extent cancel each other.

The self-exchange rate constant k_{11} of $[Ni^{III/II}(cyclam)]^{3+/2+}$ has been measured, and a value of $\sim 10^3$ M^{-1} s^{-1} is reported.[34] The self-exchange rate constant k_{22} of $[Cu^{III/II}HL^n]^{2+/+}$ is not known. The value of K_{12}, for each cross-reaction, is calculated by using the standard electrode potential $E°$, calculated from eq 4 for the Cu(III/II) couples at pH 0 (Table II), and the reported redox potential of the Ni(III/II) cyclam couple (0.97 V vs NHE).[35] In the application of the Marcus theory the value for k_3 (the second-order constant at $[H^+] = 1$ M) was used. A value for k_{22} was calculated by using the log form of eq 10 assuming $f = 1$. The value of k_{22} was then used to calculate f and k_{22} until the best fit of log k_3 vs log ($k_{11}K_{12}f$) was obtained as shown in Figure 2. This plot has a slope of 0.46, which is in reasonable agreement with the predicted value of 0.5. The self-exchange rate constant of the $[Cu^{III/II}HL^n]^{2+/+}$ couples with alkyl substituents is calculated as $\sim 5 \times 10^5$ M^{-1} s^{-1}. A value of $\sim 7 \times 10^5$ M^{-1} s^{-1} is estimated for the phenyl-substituted Cu(III/II) couple. The higher value of the self-exchange of the phenyl-substituted complexes probably results from the π system of the aromatic ring, which may facilitate electron transfer. This may explain the deviation shown by this complex from the linear free energy relationship shown in Figure 2. However, when the values of k_{22} calculated for the alkyl- and the phenyl-substituted complexes were used to plot log k_3 vs log ($k_{11}k_{22}K_{12}f$), the point falls on the line, and the linear plot has a slope of 0.46 ± 0.02 and an intercept of 0.22 ± 0.19. The involvement of the aromatic ring in electron transfer has become more evident in the reactions of $[Cu^{III}L^n]^+$ with $Co(phen)_3^{2+}$ (phen = 1,10-phenanthroline). Only the reaction involving the Cu(III) complex with the phenyl substituent was too fast to follow on the stopped-flow instrument.[17] It is to be observed that the self-exchange rate constant of the $[Cu^{III/II}HL^n]^{2+/+}$ complexes is about 1 order of magnitude higher than the self-exchange constant of the Cu(III/II) peptide complexes determined by ^1H NMR line broadening (5.5×10^4 M^{-1} s^{-1}).[36] These differences in rate, probably, reflect the small changes in Cu–N bond lengths (<0.02 Å) in the copper imine–oxime complexes compared to the large changes in the bond length (>0.1 Å) of the copper peptide complexes between the +2 and +3 oxidation states.[11] The self-exchange rate constant calculated for $[Cu^{III/II}HL^1]^{2+/+}$ was used to calculate its cross-reaction rate constant with catechol, and a fairly good agreement between the calculated ($\sim 4 \times 10^6$ M^{-2} s^{-1}) and the observed values (5.2×10^6 M^{-2} s^{-1}) was found.[17]

Acknowledgment. Financial support for this work provided by the Research Council of Kuwait University under Grant No. SC030 is greatly appreciated.

Registry No. $[Ni^{II}(cyclam)]^{2+}$, 46365-93-9; $[Cu^{III}L^1]^+$, 89230-27-3; $[Cu^{III}L^2]^+$, 117733-88-7; $[Cu^{III}L^3]^+$, 117687-05-5; $[Cu^{III}L^4]^+$, 117687-06-6.

Supplementary Material Available: A table of rate constant determinations using different Cu(III) complex concentrations and various H^+ concentrations (2 pages). Ordering information is given on any current masthead page.

(34) McAuley, A.; Macartney, D. H.; Oswald, T. *J. Chem. Soc., Chem. Commun.* **1982**, 274.
(35) Brodovitch, J. C.; McAuley, A.; Oswald, T. *Inorg. Chem.* **1982**, *21*, 3442.
(36) Koval, C. A.; Margerum, D. W. *Inorg. Chem.* **1981**, *20*, 2311.

Contribution from the Departamento de Química Inorgánica, Facultad de Farmacia, Universidad de Valencia, 46010 Valencia, Spain, and Institut de Ciència de Materials, CSIC Barcelona, Barcelona, Spain

Coordination Behavior of Acetazolamide (5-Acetamido-1,3,4-thiadiazole-2-sulfonamide): Synthesis, Crystal Structure, and Properties of Bis(acetazolamidato)tetraamminenickel(II)

S. Ferrer,† J. Borrás,*,† C. Miratvilles,‡ and A. Fuertes‡

Received April 23, 1988

Acetazolamide (Acm) (Figure 1) is one of the most potent inhibitors of carbonic anhydrase enzyme.[1] It is used as a diuretic drug and in the treatment of glaucoma. Although the mechanism whereby Acm inhibits the carbonic anhydrase is not well understood, direct binding studies using $[^3H]$Acm showed that Acm acts by coordinating the Zn atom of the active site. The $-SO_2-NH_2-$ seems to be the obvious candidate as the metal-chelating group.[2] The sulfonamide N atom must occupy the fourth coordination site at the Zn environment, replacing the Zn-bound water molecule in the native enzyme. One oxygen atom of the sulfonamide group links weakly the metal to give a distorted (4 + 1) "tetrahedron".[3]

We have initiated studies on the coordination chemistry of Acm and derivatives with transition-metal and d^{10} metal ions in an attempt to examine their mode of binding. As this ligand possesses the both character of thiadiazolyl and sulfonamide derivatives, a goal of our current investigation is the understanding of the coordination behavior of a compound with both groups. We have reported previously the synthesis and characterization of $M(Acm)_2(NH_3)_2$ (M = Zn or Co).[4] The complex described here is the first structurally characterized complex of Acm.

Finally, the crystal structure of this complex allows us to know where the deprotonation of the Acm takes place, since the literature indicates there are two ionizable hydrogens in the Acm, but

*To whom correspondence should be addressed.
†Universidad de Valencia.
‡CSIC Barcelona.

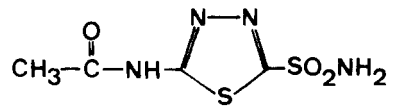

Figure I. Acetazolamide.

Table I. Physical Properties and Main Data Relating to Measurement and Refinement of Structure

1. Physical and Crystallographic Properties	
formula	$C_8H_{22}NiN_{12}O_6S_4$
mol wt	569.3
cryst syst	triclinic
space group	$P\bar{1}$
Z	1
cell consts	a = 7.525 (3) Å, b = 8.690 (3) Å, c = 8.795 (8) Å, α = 83.89 (5)°, β = 76.81 (5)°, γ = 83.09 (3)°
vol	554 (1) Å^3
ρ_{calcd}	1.71 g·cm^{-3}
$\mu_{Mo K\alpha}$	12.53 cm^{-1}
cryst shape	prismatic (0.14 × 0.15 × 0.18 mm)
2. Data Pertinent to Measurement	
temp	293 K
radiation	λ(Mo Kα) = 0.70926 Å
monochromator	graphite
takeoff angle	12.0°
cryst–detector dist	173 mm
detector aperture	4 mm × (2.4 + 1.05 tan θ) mm
scan type	$\omega/2\theta$
scan width	(0.8 + 0.34 tan θ)°
θ range	1–25°
std reflcns	
intensity (period 1 h)	(2,2,2)
orientation (period 50 reflcns)	(1,3,2), (2,5,4), (1,5,4)
no. of reflcns measd	2112
3. Data Treatment and Refinement	
no. of reflcns used with $I > 2.5\sigma_I$	NO = 1550
no. of variables	NV = 176
weighting scheme	$w = 1/(\sigma^2(F_o) + 0.010711F_o^2)$
agreement factors	
$R = (\sum\|\|F_o\| - \|F_c\|\|)/(\sum\|F_o\|)$	0.069
$R_w = [\sum w(\|F_o\| - \|F_c\|)^2/\sum w\|F_o\|^2]^{1/2}$	0.098
$s = [\sum w(\|F_o\| - \|F_c\|)^2/(NO - NV)]^{1/2}$	2.7

there is no reported evidence to demonstrate which proton is more acidic.

Experimental Section

Synthesis. Violet prismatic crystals were obtained by dissolving 2.200 g of Acm powder in a boiling solution of $Ni(ClO_4)_2$ (2 mmol) in EtOH (200 mL). After that, 30 mL of concentrated ammonia was added dropwise with stirring. Then, the violet precipitate that appeared was redissolved by adding the necessary volume of concentrated ammonia (approximately 20 mL) to give a beautiful clear violet solution. Crystals were formed by cooling and by a slow room-temperature evaporation of that resulting solution after a period of several days. Anal. Calcd for $C_8H_{22}N_{12}O_6S_4Ni$: C, 16.9; H, 3.9; N, 29.5; Ni, 10.3. Found: C, 16.9; H, 3.8; N, 29.5; Ni, 10.3.

Crystallographic Data Collection and Refinement of the Structure. The crystal used was violet with a prismatic shape. The X-ray data were recorded with a CAD-4 Enraf-Nonius diffractometer by using graphite-monochromated Mo Kα radiation. Cell dimensions were obtained by a least-squares fit from the setting angles of 25 well-centered reflections with 12° ≤ θ ≤ 25°. Information concerning conditions for crystallographic data collection and structure refinement is summarized in Table I. Lorentz and polarization corrections were applied, but not for absorption. The space group $P\bar{1}$ was assumed throughout the structure analysis and was confirmed by the successful refinement of the structure. The positions of nickel and eight non-hydrogen atoms were determined by direct methods (MULTAN 11/84).[5] The remaining non-hydrogen atoms

Table II. Positional Parameters[a]

	x/a	y/b	z/c
Ni	0	0	0
S(1)	516 (2)	−2974 (2)	4711 (2)
S(2)	−3317 (2)	−1611 (2)	6315 (2)
O(1)	3668 (6)	−4338 (5)	3830 (5)
O(2)	−2686 (6)	−2520 (5)	7579 (5)
O(3)	−3905 (6)	1 (5)	6463 (5)
N(1)	−1548 (6)	−940 (6)	3372 (5)
N(2)	14 (7)	−1254 (6)	2241 (5)
N(3)	2859 (7)	−2745 (6)	1796 (5)
N(4)	−4971 (7)	−2410 (6)	5944 (6)
N(5)	−2788 (7)	−244 (6)	268 (6)
N(6)	827 (7)	−2087 (6)	−1126 (6)
C(1)	−1446 (8)	−1746 (7)	4691 (6)
C(3)	4009 (8)	−3752 (7)	2456 (7)
C(2)	1243 (8)	−2304 (6)	2732 (6)
C(4)	5887 (11)	−4181 (9)	1468 (9)

[a] Multiplied by 10^4.

Table III. Bond Distances and Angles

Distances (Å)			
N(2)–Ni	2.150 (5)	C(1)–S(2)	1.765 (5)
N(5)–Ni	2.091 (5)	C(3)–O(1)	1.242 (7)
N(6)–Ni	2.118 (5)	N(2)–N(1)	1.376 (6)
C(1)–S(1)	1.717 (6)	C(1)–N(1)	1.302 (8)
C(2)–S(1)	1.759 (5)	C(2)–N(2)	1.330 (7)
O(2)–S(2)	1.431 (4)	C(3)–N(3)	1.338 (7)
O(3)–S(2)	1.428 (5)	C(2)–N(3)	1.342 (8)
N(4)–S(2)	1.606 (5)	C(4)–C(3)	1.508 (9)
Angles (deg)			
N(5)–Ni–N(2)	90.8 (2)	C(2)–N(2)–Ni	131.8 (4)
N(6)–Ni–N(2)	90.5 (2)	C(2)–N(2)–N(1)	113.8 (5)
N(6)–Ni–N(5)	93.0 (2)	C(2)–N(3)–C(3)	116.3 (5)
C(2)–S(1)–C(1)	86.3 (3)	S(2)–C(1)–S(1)	123.3 (3)
O(3)–S(2)–O(2)	119.1 (3)	N(1)–C(1)–S(1)	116.7 (4)
N(4)–S(2)–O(2)	108.6 (3)	N(1)–C(1)–S(2)	119.9 (4)
N(4)–S(2)–O(3)	107.7 (3)	N(3)–C(3)–O(1)	125.2 (6)
C(1)–S(2)–O(2)	105.1 (3)	C(4)–C(3)–O(1)	117.3 (6)
C(1)–S(2)–O(3)	107.5 (3)	C(4)–C(3)–N(3)	117.5 (6)
C(1)–S(2)–N(4)	108.4 (3)	N(2)–C(2)–S(1)	112.3 (4)
C(1)–N(1)–N(2)	110.9 (5)	N(3)–C(2)–S(1)	125.4 (4)
N(1)–N(2)–Ni	114.4 (4)	N(3)–C(2)–N(2)	122.2 (5)

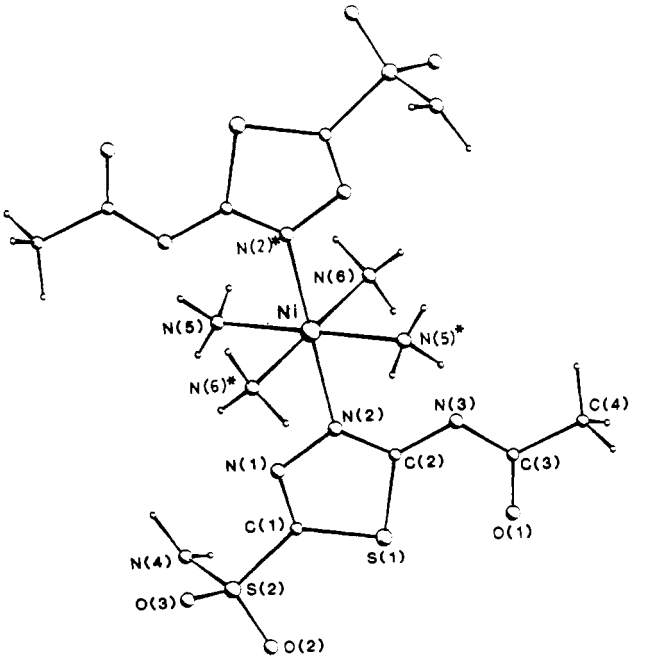

Figure 2. Perspective view of $[Ni(Acm)_2(NH_3)_4]$.

(1) Miller, W. H.; Dessert, A. M.; Roblin, R. O., Jr. *J. Am. Chem. Soc.* **1950**, *72*, 4893.
(2) Brown, R. S.; Huguet, J.; Curtis, N. J. Models for Zn(II) binding in enzymes. In *Metal Ions in Biological Systems*; Sigel, H., Ed.; Marcel Dekker: New York, 1983; Vol. 15.
(3) Vedani, A.; Dunitz, J. D. *J. Am. Chem. Soc.* **1985**, *107*, 7653.
(4) Ferrer, S.; Jimenez, A.; Borrás, J. *Inorg. Chim. Acta* **1987**, *129*, 103.

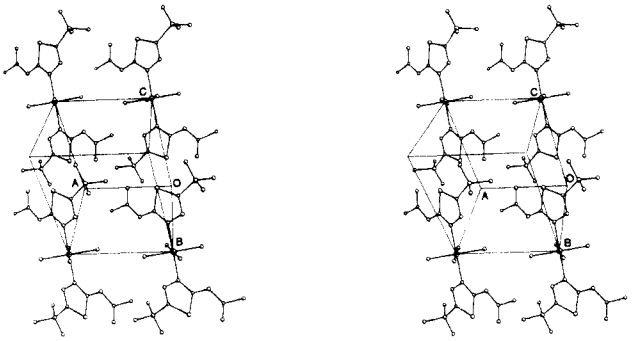

Figure 3. Stereoscopic view of the unit cell showing four discrete units of $[Ni(Acm)_2(NH_3)_4]$.

were located from successive Fourier Syntheses. Refinement of the structure was carried out with the SHELX 76 system[6] by weighted anisotropic full-matrix least-squares methods. Positions of all hydrogen atoms present in the molecule were determined by Fourier difference syntheses and included in the final refinement with common fixed isotropic thermal parameters (U = 0.062 Å^2). In the final difference map the residual maximum was a peak of 1.2 e Å^{-3} located near the nickel atom. Atomic scattering factors and corrections for anomalous dispersion for Ni atom were taken from ref 7. The geometrical calculations were performed with XANADU[8] and DISTAN,[9] and molecular illustrations were drawn with PLUTO.[10] Atomic parameters are given in Table II. Bond lengths and bond angles are tabulated in Table III.

Results and Discussion

Figure 2 shows a perspective view of the molecule and the atom labeling; a stereoscopic view of the unit cell contents is given in Figure 3.

Coordination Polyhedron. The structure consist of discrete units of $[Ni(Acm)_2(NH_3)_4]$ that interact only through van der Waals contacts and hydrogen bonds. The Ni(II) ions, lying on symmetry centers, are bonded to six nitrogen atoms, forming NiN_6 chromophores in a slightly elongated rhombically distorted octahedral environment. The equatorial plane is formed by the four ammonia N atoms and the axial positions are occupied by two thiadiazole N atoms [N(2)] from different trans ligand molecules. The small difference between the Ni–$N_{ammonia}$ and Ni–N(2) distances (Ni–$N_{ammonia}$ (av) = 2.105 (7) Å; Ni–N(2) = 2.150(5) Å) arises from the steric hindrance that the bulk axial Acm ligands (essentially the acetamido moiety) produce with the ammonia molecules. In fact, the nearly planar Acm molecules approximate to the nickel atom through a plane that roughly bisects the N(5)–Ni–N(6)* angle in order to minimize the Ni–N(2) distance in turn to avoid the shorter N(3)–ammonia distances that otherwise would be produced. On the other hand, the slightly smaller observed Ni–N(5) distance, compared to Ni–N(6), is related to the fact that N(5) but not N(6) is hydrogen bonded to the acetamido deprotonated nitrogen atom N(3) (see below). The steric hindrance from this atom to the N(6) ammonia molecule is also reflected in the angle Ni–N(2)–C(2) (131.8 (4)°), which is significantly greater than Ni–N(2)–N(1) (114.4 (4)°).

Ligand Conformation and Crystal Packing. A comparison between the previously determined structure of Acm[11] and the structure of this ligand in the Ni(II) complex shows several interesting aspects. The N(1)–N(2) distance in the complex [1.376 (6) Å] is comparable to that found in the ligand [1.372 (3) Å], indicating that the bond between N(2) and the Ni(II) ion has no influence in this length. The N(2)–C(2) distance is a little longer in the complex [1.330 (7) Å] than in free Acm [1.311 (3) Å]. This reduction of the N(2)–C(2) bond order appears to be related to the more important increase of the C(2)–N(3) bond order. The more interesting changes correspond to the acetamido group. Both C(2)–N(3) and N(3)–C(3) bond lengths are shorter in the title compound [1.342 (8) and 1.338 (7) Å for the complex; 1.369 (3) and 1.355 (3) Å for the ligand, respectively] owing to a bigger electronic density. Furthermore, the C(3)–O(1) distance increases in the complex [1.222 (2)–1.242 (7) Å]. All these effects must take place because of the deprotonation of the acetamido group.

As far as the C–S distances is concerned, the most significant feature is that while in the Acm the two C–S bond lengths in the thiadiazole ring were similar, the C(2)–S(1) bond changes from 1.724 (2) Å in the Acm to 1.759 (5) Å in the complex, while the C(1)–S(1) bond remains quite unchanged (from 1.730 (3) to 1.717 (6) Å). The C–S bond lengths in the thiadiazole ring are significantly shorter than the commonly accepted values of 1.80 Å for a C–S single bond or 1.77 Å for a C(sp^2)–S single bond. Thus, the lower distances in the Acm ring have some double-bond character resulting from the delocalization in the thiadiazole ring. Since in the complex C(2)–S(1) is closer to a C–S single bond, it can be inferred that is has had a redistribution of the negative charge.

The sulfonamido group remains significantly unchanged in the complex. The C(1)–S(2), S(2)–O(2), and S(2)–O(3) distances are similar to their equivalents in Acm as expected since there is no interaction between the metal ion and the sulfonamido group. Only the S(2)–N(4) bond length has suffered a small increase [1.594 (3) to 1.606 (5) Å], which must be related to the changes in the hydrogen-bonding system. As has been noted, the ligand atoms, except the oxygen and nitrogen atoms from this group, lie in the title compound approximately on a plane that nearly bisects the N(5)–Ni–N(6)* angle (mean plane S(2)C(1)N(1)N(2)C(2)S(1)N(3)O(1)C(3)C(4); root-mean-square deviation, 0.03 Å. Distances to plane: Ni, 0.03 Å; N(5), –1.28 Å; N(6)*, 1.60 Å), and is roughly perpendicular (90.3°) to the plane formed by the nickel atom and the four ammonia molecules.

Each $[Ni(Acm)_2(NH_3)_4]$ molecule interacts with three other molecules through an extensive network of hydrogen bonds involving ammonia molecules, the $-NH_2$ group, and oxygen atoms from the sulfonamido moiety (see Table IV). There is also an intramolecular hydrogen between the ammonia molecule N(5) and the deprotonated N(3) atom from the ligand, which may account for the different coordinating behavior of the two ammonia molecules with the nickel atom.

Properties. The complex exhibits characteristic IR spectra due to ligand vibration modes. The most significant IR bands are

Table IV. Hydrogen Bonds

A–H···B[a]	H···B, Å	A···B, Å	A–H···B, deg
N(4)–H(N41)···O(1)^{i}	2.05 (7)	2.880 (6)	172 (4)
N(4)–H(N42)···O(3)^{ii}	1.93 (7)	3.004 (6)	164 (4)
N(5)–H(N51)···O(2)^{iii}	2.20 (7)	3.223 (6)	157 (4)
N(5)–H(N52)···O(3)^{ii}	2.59 (7)	3.352 (6)	162 (4)
N(5)–H(N53)···N(3)^{iv}	2.06 (7)	3.009 (6)	147 (4)
N(6)–H(N61)···O(2)^{iii}	2.14 (7)	3.183 (6)	166 (4)

[a] The second atom (B) is related to the atom listed in Table II by the following symmetry operations: (i) $-x, -1-y, 1-z$; (ii) $-1-x, -y, 1-z$; (iii) $x, y, z-1$; (iv) $-x, -y, -z$.

Table V. Selected IR Frequencies (cm^{-1}) for Acetazolamide and Acetazolamide–Metal Complexes[a]

compd	ν(C=O)	$\nu_{as}(SO_2)$	$\nu_s(SO_2)$
Acm	1672 s	1318 s	1170 s
$Zn(Acm)_2(NH_3)_2$	1699 s	1285 s	1145 s
$Co(Acm)_2(NH_3)_2$	1705 s	1290 s	1145 s
$Ni(Acm)_2(NH_3)_4$	1681 w, 1624 m	1328 s	1178 s

[a] Key: w = weak, m = medium, s = strong.

(5) Main, P.; Germain, G.; Woolfson, M. M. "MULTAN 11/84, A System of Computer Programs for the Automatic Solutions of Crystal Structures from X-ray Diffraction Data"; Universities of York, U.K., and Louvain, Belgium, 1984.
(6) Sheldrick, G. M. "SHELX 76, Program for Crystal Structure Determination"; University of Cambridge, U.K., 1976.
(7) *International Tables for X-ray Crystallography*; Kynoch Press: Birmingham, U.K., 1974; Vol. 1, pp 72 and 99.
(8) Roberts, P.; Sheldrick, G. M. "XANADU, Program for Crystallographic Calculations"; University of Cambridge, U.K., 1975.
(9) Burzlaff, L.; Böhme, V.; Gomm, M. "DISTAN"; University of Erlängen, Federal Republic of Germany, 1977.
(10) Motherwell, W. D. S.; Clegg, W. "PLUTO 78, Program for Plotting Molecular and Crystal Structures"; University of Cambridge, U.K., 1978.
(11) Mathew, M.; Palenik, G. J. *J. Chem. Soc., Perkin Trans. 2* **1974**, 532.

Table VI. Spectral Data and Conductance Measurements[a]

	λ_{max}, cm^{-1} (ϵ_{max}, M^{-1} cm^{-1})		
	ν_2	ν_3	Λ_M,[b] Ω^{-1} cm^2 mol^{-1}
solid	17857	28329 sh	
H_2O	15503 (6)	26315 sh	213
DMSO	15673 (7)	26315 sh	26
DMF	15389 (11)	25000 sh	21

[a] sh = shoulder. [b] At 298 K.

shown in Table V. Since in the title compound there are several C=N and N—H groups (from the Acm and from the ammonia) the correspondent IR bands do not give information about which groups have been modified. The first significant difference between the IR spectrum of the present complex and those of the previously cited complexes concerns the splitting of the absorption frequencies of the carbonyl group. While the Zn and Co complexes present a very strong band at higher frequencies than in Acm, the Ni complex shows a very weak band at 1681 cm^{-1} and a medium one at 1624 cm^{-1}. This is a consequence of the deprotonation of the acetamido group, resulting in a delocalization of the negative charge on the carbonyl double bond by way of several resonance forms and leading to a great reduction of the C=O bond order. The longer C=O bond length and the shorter C—N bond length of the acetamido group in the complex compared with the same bond length in the Acm structure are in agreement with the IR results.

Although from the IR data it could be inferred that the coordination takes place through the carbonyl group, the crystal structure shows that the change in this stretching vibration is due to the deprotonation. On the other hand, the asymmetric and symmetric stretching vibrations of the SO_2 group have not changed in comparison to those of the free ligand. This indicates that there is no interaction between the sulfonamido group and the metal ion, which is also confirmed by the X-ray analysis. In the Zn and Co complexes, this bands are shifted to lower frequencies, suggesting a different mode of coordination, which the sulfonamido group is involved in.

From the crystal structure of the Ni complex it could be said that the more acidic proton of the Acm is the amido one; however, the behavior of that ligand does not have to be similar in complexes with other ions. So, in the Zn and Co complexes the spectroscopic data evidence that deprotonation takes place in the sulfonamido group. In addition, the crystal structure of a Cu(II) complex, which will be reported later, shows the ligand with a double deprotonation.

The solid d-d spectrum shows three characteristic bands of Ni(II) in an octahedral environment. The B and $10Dq$ values (1080 and 10840 cm^{-1}, respectively) fall within the range observed for a NiN_6 chromophore.[12] The room-temperature magnetic moment calculated by the Faraday method (3.21 μ_B) represents the usual behavior for a mononuclear and distorted octahedral Ni(II) complex. The reflectance spectrum and the magnetic data are in agreement with the X-ray results.

The solid compound and its aqueous, dimethyl sulfoxide, and N,N'-dimethylformamide solutions have different colors and electronic spectra, and thus, we would expect a different chromophore. Nevertheless, the spectral data (see Table VI) indicate an octahedral environment. These results and the conductance measurements suggest that solvent molecules replace the ligand in the Ni(II) coordination sphere.

Acknowledgment. We greatly appreciate financial support from the Comisión Asesora de Investigación Científica y Técnica, Spain (Grant 932/84).

Supplementary Material Available: Tables of equations of least-squares planes, fractional coordinates for hydrogen atoms, and anisotropic thermal parameters (3 pages); a table of observed and calculated structure factors (5 pages). Ordering information is given on any current masthead page.

(12) Lever, A. B. P. *Inorganic Electronic Spectroscopy*, 2nd ed.; Elsevier: Amsterdam, 1984.

Contribution from the Department of Physical and Inorganic Chemistry, University of Western Australia, Nedlands, Western Australia, Australia 6009

Lewis Base Adducts of Main Group 1 Metal Compounds. 7.† The Lithium–Coinage-Metal Parallel: Novel Adducts of Lithium(I) Bromide and Iodide with 2,6-Dimethylpyridine

Colin L. Raston,[1] Claire R. Whitaker, and Allan H. White*

Received April 22, 1988

Copper(I) halides, CuX (X = Cl, Br, I), with monodentate nitrogen bases, L, yield adducts of stoichiometry $XCuL_n$, chiefly for n = 1–3, exhibiting a variety of oligomeric and polymeric forms,[2] over which some control may be exercised by the stoichiometry of the reaction conditions and the steric profile of the ligand. With silver(I),[3] as the consequence of a change in balance between solvation and lattice energies, the higher values of n become much more difficult to access, while the isomeric possibilities found in the copper system are much more restricted but with new forms emerging, as the consequence of both energetic considerations and the larger size of silver(I). In this context, our recent studies with lithium(I),[4,5] demonstrating, perhaps surprisingly, characteristics with respect to complex formation intermediate between those of copper(I) and silver(I) by virtue of the formation of species of high n, but with a metal radius nearer that of silver(I), emerge with considerable novelty. Recrystallization of the lithium halides from 3,5-dimethylpyridine (3,5-dmpy) yields the mononuclear series of four-coordinate species $[XLiL_3]$[5,6] paralleling the previously characterized copper(I) series, while similar parallel series are found with 2-methylpyridine (2-mpy) as the binuclear arrays $L_2MX_2ML_2$ (M = Cu,[7] Li;[5] X = all Cl, Br, I). With 2,6-dimethylpyridine (2,6-dmpy), recrystallization of CuX yields mononuclear, three-coordinate L_2CuX.[8,9]

Recrystallization of the copper(I) halides from the parent base is usually readily accomplished, providing air is excluded; with lithium the (more difficult) problem is the total exclusion of moisture, and we find the formation of crystalline lithium(I) halide–nitrogen base adducts a more difficult procedure. In attempting the synthesis of adducts with 2,6-dmpy, we have thus far achieved success only with the bromide and iodide, obtaining complexes characterized by analysis and single-crystal structure determination as 1:1.5 and 1:2 species, respectively.

The iodide is a 1:2 complex, but, unlike its copper(I) counterpart,[8] it is a binuclear, centrosymmetric $L_2LiI_2LiL_2$ species, the first binuclear species of this type obtained with this ligand, presumably a consequence of the increased size of lithium(I) vs that of copper(I). (Note, however, that the relation is not simple: in $[(3,5\text{-dmpy})_3MX]$, for X = Cl, Br, I, M–X distances are 2.320 (9), 2.51 (2), and 2.80 (1) Å for M = Li[4] and 2.412 (9), 2.51 (1), and 2.683 (3) Å for M = Cu![6]). Geometries of the $N_2LiI_2LiN_2$ (L = 2-mpy,[5] 2,6-dmpy) and $N_2CuI_2CuN_2$ (L = 2-mpy[7]) systems are compared in Table II. We note the generally increased Li–N and Li–I distances in the 2,6-dmpy complex, and in this complex the I–M–N angles are divided into two sets, ca. 95 and 134°, suggestive of the presence of steric strain in the 2,6-dmpy adduct, as might be expected. The ligand disposition may be compared with that of unstrained $[(3,5\text{-dmpy})_2CuI_2Cu(3,5\text{-dmpy})_2]$,[8] which adopts almost perfect *mmm* symmetry. With 2,6-substituents maximum symmetry may be achieved by cleavage of the dimer to a monomer with concomitant opening of the N–Cu–N ring angle to ca. 150°—this disposition with incipient *2mm* symmetry is found in both forms of $[(2,6\text{-dmpy})_2CuI]$.[8] Alternatively, the dimer may be preserved with loss of symmetry to diminish interactions between the methyl groups on ligands *gem* to the same metal; this is achieved by a twist of the N_2M planes about the M···M axis so that they no longer lie normal to the MX_2M plane.

† Part 6: Raston, C. L.; Whitaker, C. R.; White, A. H. *Aust. J. Chem.* **1988**, *41*, 413.

0020-1669/89/1328-0163$01.50/0